Assessment of Land Surface Temperature Dynamics of Chamoli District Using Landsat Data: Implications for Vegetation Cover Monitoring

Uma Bhattacharya[1], Rajesh Jolly[2]

[1]Research Scholar, Department of Geography, Lovely Professional University, Phagwara 144411, Punjab, India
[2]Associate Professor, Department of Geography, Lovely Professional University, Phagwara 144411, Punjab, India

Abstract
Thermal infrared remote sensing data is vital for analyzing and mapping Land Surface Temperature (LST), allowing for the capture of apparent surface temperature through radiant energy. The use of ArcGIS software simplifies the calculation of LST. Landsat-8, and Thermal Infrared Sensor (TIRS) data with 100 m resolution have been used for the calculation of LST of the study area. Landsat 5-8 data has been taken to understand the seasonal comparison and yearly changes in LST. OLI Band 4, and 5 have been used for the calculation of the Normalized Difference Vegetation Index (NDVI). The ultimate result shows that the surface temperature was low in the densely vegetated areas, while it was high for the barren land. Satellite data from 2000 to 2025 for winter, summer, and monsoon was compared to assess the changes in the surface emissivity. An integrated approach has been taken for the mapping and monitoring of forest resources of the study area with the help of LST data and other indices, i.e., NDVI and NDWI. This integrated approach enables the identification of areas susceptible to stressors like drought, pest infestation, and land degradation, facilitating proactive management interventions.

Keywords: Land Surface Temperature, Single Window Algorithm, NDVI, OLI, TIRS

Introduction

One of the biggest environmental problems that people are currently dealing with is how these factors impact people worldwide and increase their dependence on necessities. There is a lack of focus on some area in the research depicting the connection between environmental causes and land surface temperature (LST). The surface temperature and the physical characteristics of the land surface are directly correlated. Accordingly, for high-altitude mountain landscapes, the Normalized Difference Vegetation Index (NDVI) is the best instrument for measuring Land Surface Temperature (LST) (S Suresh et. al, 2016). One important variable and radiation transmission in the atmosphere is land surface temperature (LST), which is measured via remote sensing and GIS (P Rajendran et. al, 2015). The land use and land cover analysis plays a crucial role for the estimation of land surface temperature analysis. The physical state, vegetation cover, and anthropogenic activities of a place are all directly correlated with the land surface temperature (LST). Local climate also has impact of the surface temperature. The conventional method for figuring out the surface temperature and its slow variations is to analysing the climatic data collected from the meteorological department of any other observatories. Landsat OLI-TIRS data from band 9 to band 11 (1-9 with 30m resolution, and 10-11 with 100 m resolution) has been collected form USGS site for this current study.

Land Surface Temperature (LST) is the "skin" temperature of the Earth's surface, representing how hot the land surfaces are at any given moment. LST is crucial for understanding the exchange of energy and water between the land surface and the atmosphere. Land Surface Temperature (LST) is defined as a measure of how hot or cold the Earth's surface would feel to the touch. It is the temperature of the "skin" of the ground, and it is mainly influenced by albedo, vegetation cover, and soil moisture. From a satellite's perspective, the "surface" can refer to snow, ice, grass, building roofs, or forest canopies. LST differs from the air temperature reported in daily weather forecasts. This temperature is a key indicator of the surface energy budget, impacting the net radiation balance and supporting various fields like hydrology, meteorology, and climatology. It also affects the rate and timing of plant growth. LST measurements are essential for monitoring crop and vegetation health, assessing thermal stress, and understanding energy exchanges between the land and atmosphere.

Objectives of the Study

The objectives of the current study are as follows:
To analyze temporal trends and spatial variability of Land Surface Temperature (LST) in Chamoli District during summer seasons from 1990 to 2025 using Landsat satellite data.
To assess the impact of LST dynamics on local vegetation cover changes

Location of the Study Area:

Chamoli district, located in the state of Uttarakhand, India (fig 1), is part of the central Himalayas, renowned for its rich biodiversity, cultural heritage, and scenic landscapes. However, the region's rugged terrain and fragile ecosystem also make it particularly vulnerable to natural hazards such as landslides, earthquakes, floods, and glacial lake outburst floods (GLOFs). This chapter examines the geoenvironmental setting of Chamoli and evaluates its susceptibility to these hazards, providing a foundation for understanding the broader context of land

cover change and hazard management. Chamoli covers an area of approximately **8,030 square kilometers**, with its terrain defined by towering Himalayan peaks, steep slopes, deep valleys, and glacial rivers. The district lies between **latitude 30°15'N to 31°5'N** and **longitude 79°05'E to 80°30'E**, and includes significant peaks like **Nanda Devi** (7,816 meters) and **Trishul** (7,120 meters). The region's geology is characterized by **Precambrian metamorphic rocks**, such as schists, gneisses, and quartzites, intersected by tectonic fault lines, particularly the **Main Central Thrust (MCT)**. The active tectonic setting contributes to the region's high seismicity, exemplified by the **1999 Chamoli earthquake (magnitude 6.8)**. Located in Seismic Zone V, Chamoli is highly susceptible to earthquakes due to the active tectonic setting. The melting of glaciers and intense monsoons increase the risk of glacial lake outburst floods (GLOFs) and flash floods. The high-altitude regions experience frequent avalanches during winter due to heavy snow accumulation. Chamoli experiences a **temperate to alpine climate**, with large variations in temperature and precipitation driven by altitude. The district receives most of its annual rainfall (ranging from **1,500 to 2,500 mm**) during the monsoon season. Heavy snowfall in winter, especially in areas above 3,000 meters, further adds to the hydrological complexity of the region. The Alaknanda River and its tributaries dominate Chamoli's hydrology, making the area prone to flash floods and rapid snowmelt-induced flooding.

Fig 1.

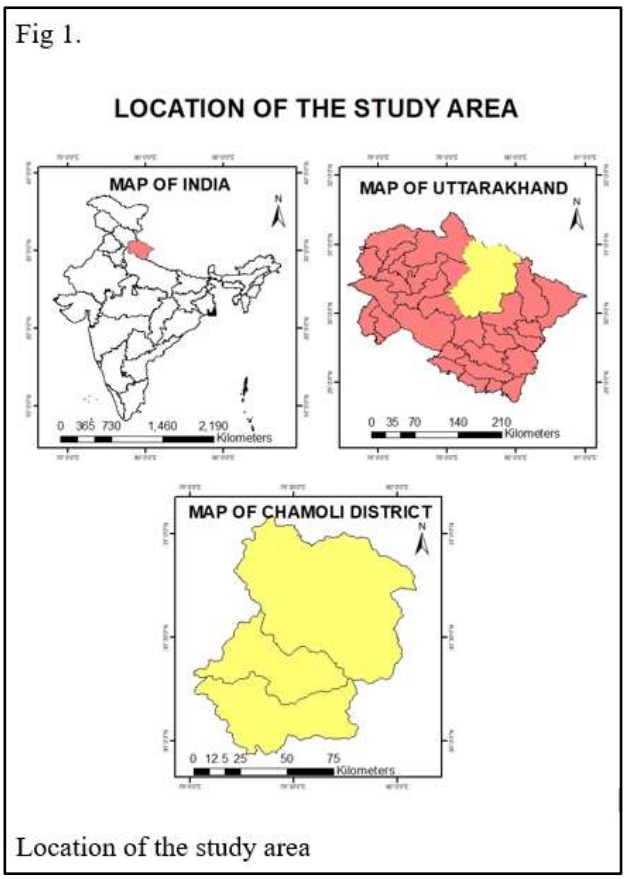

Location of the study area

Review of Literature

Land Surface Temperature (LST) Calculation and Remote Sensing Techniques:

Land Surface Temperature is taken as a critical parameter for the intensive study of climate change, earths surface energy balance, study of urban heat island, etc. Various techniques and algorithms have been developed to retrieve accurate LST from satellite data, leveraging the advancements in sensor technology and image processing algorithms. Thermal infrared remote sensing is one of the primary methods used for LST retrieval. The study by Sun and Pinker (2003) highlighted the estimation of LST from the Geostationary Operational Environmental Satellite (GOES-8), demonstrating the effectiveness of satellite data in capturing thermal characteristics of the Earth's surface. Similarly, the work of Anderson et al. (2008) showcased a thermal-based remote sensing technique that enables the routine mapping of land-surface carbon, water, and energy fluxes, underscoring the versatility of thermal infrared data in environmental monitoring (Anderson et al., 2008). These methods often require validation against ground measurements to ensure accuracy, as demonstrated by Coll et al. (2005), who validated LST derived from AATSR and MODIS data using ground measurements (Coll et al., 2005).

Key algorithms like the split-window technique and the Surface Energy Balance Algorithm for Land (SEBAL) have been instrumental in LST retrieval. The split-window algorithm, evaluated by Coll et al. (2006), uses the differential absorption of thermal infrared radiation in two adjacent spectral bands to estimate LST (Coll et al., 2006). Du et al. (2015) further advanced this approach with a practical algorithm for estimating LST from Landsat 8 data, which has become widely used due to its accessibility and high-resolution thermal data (Du et al., 2015). On the other hand, the SEBAL formulation developed by Bastiaanssen et al. (1998) integrates remote sensing data with a surface energy balance model to derive LST and other surface parameters (Bastiaanssen et al., 1998).

The integration of machine learning techniques has also enriched LST retrieval methods. Aires et al. (2001) introduced a neural network approach that incorporates a first guess for retrieving surface temperature and emissivities from satellite microwave observations, showcasing the potential of artificial intelligence in enhancing remote sensing data accuracy (Aires et al., 2001). Moreover, the System for Automated Geoscientific Analyses (SAGA) developed by Conrad et al. (2015) provides a robust platform for processing and analyzing geospatial data, supporting the automated retrieval of LST and other parameters (Conrad et al., 2015).

Validation with in-situ measurements remains crucial for ensuring the reliability of satellite-derived LST. Duan et al. (2019) emphasized this through their validation of the MODIS LST product, highlighting discrepancies that can occur and the importance of continuous validation efforts (Duan et al., 2019). Similarly, Jackson et al. (1981) utilized canopy temperature as an indicator of crop water stress, demonstrating the applicability of LST in agricultural monitoring and the importance of accurate LST data (Jackson et al., 1981).

Urban heat island studies have particularly benefited from thermal remote sensing. Voogt and Oke (2003) reviewed the thermal remote sensing of urban climates, pointing to its effectiveness in capturing temperature variations related to urbanization (Voogt & Oke, 2003). Weng et al. (2004; 2009) further explored the relationship between LST and vegetation abundance in urban areas, using remote sensing to better understand and mitigate urban heat island effects (Weng et al., 2004; 2009).

In practice, these techniques have been applied to various regional studies. For instance, Suresh et al. (2015) analyzed LST variations in Devikulam Taluk, Kerala, India, leveraging Landsat satellite data to understand local thermal patterns (Suresh et al., 2015). Similarly, Sajib and Wang (2020) compared four algorithms for estimating LST in an agricultural region of Bangladesh, providing insights into the effectiveness of different methods in varied landscapes (Sajib & Wang, 2020). Zhi-qiang and Qi-gang (2011) also demonstrated the utility of Landsat images in studying land cover and LST changes, highlighting the adaptability of remote sensing techniques across different geographic settings (Zhi-qiang & Qi-gang, 2011).

Overall, the body of literature underscores the critical role of remote sensing techniques in LST calculation. Through continuous refinement of algorithms and validation processes, these methods provide essential insights into environmental monitoring, urban planning, and climate studies, thereby supporting informed decision-making in managing and mitigating temperature-related challenges.

Vegetation Indices and Land Cover Change:

The assessment of Land Surface Temperature (LST) is intricately linked to vegetation indices and land cover changes, with remote sensing techniques offering valuable tools for this analysis. Key indices like the Normalized Difference Vegetation Index (NDVI) and the Normalized Difference Built-Up Index (NDBI) are critical in monitoring and assessing these changes. The NDVI, a widely used indicator developed for estimating vegetation health and coverage (Crippen, 1990), plays a pivotal role in understanding land cover dynamics. By measuring the density and health of vegetation, NDVI helps in discerning the extent and impact of vegetative cover on LST. For instance, Huang et al. (2020) provide an extensive review of NDVI applications in various remote sensing studies, highlighting its significance in the era of advanced satellite technology. Similarly, the study by Cantika et al. (2020) examined the effects of NDVI and NDBI on LST in Cirebon City, Indonesia, revealing the inverse relationship between vegetation cover (high NDVI) and surface temperatures, whereas increased built-up areas (higher NDBI) corresponded to elevated LST (Cantika et al., 2020).

The role of NDBI is crucial for mapping urban areas and understanding their thermal impacts. The normalized difference build-up index has been refined over the years to improve accuracy and automation in urban mapping (Chunyang He et al., 2010; Zha et al., 2003). In heavily urbanized and rapidly developing regions, such as Lagos metropolis, Nigeria, studies like that of Alademomi et al. (2022) illustrate the intertwined relationships between LST, NDVI, NDBI, and urban expansion. Their findings underscore how land cover changes in rapidly urbanizing areas significantly influence local climate patterns, particularly through the urban heat island effect.

Further, other indices like the Normalized Difference Water Index (NDWI) have been introduced to monitor water content in vegetation, providing a more nuanced understanding of plant water stress and its implications on LST. Gao (1996) outlined the NDWI's application in assessing vegetation liquid water from satellite data, which is instrumental in drought-prone areas for monitoring plant health and predicting climate impacts. Land cover changes due to human activities have been documented across various geographical settings, showcasing both positive and negative impacts on the environment. Chen et al. (2019) highlighted that both China and India have increased their green cover through conscious land-use management, contributing significantly to the global greening effort. This greening potentially mitigates some of the adverse effects of urbanization by reducing LST through enhanced vegetation cover.

From a methodological perspective, assessing these indices and their relationship with LST necessitates robust data retrieval and analysis techniques. For example, remote sensing tools like those described by Kogan (2001) for global vegetation assessment, and the operational models for surface heat flux retrieval discussed by Zhang et al. (2008), have significantly advanced the ability to monitor and analyze these parameters accurately. Niclòs et al. (2009) provided preliminary results on LST retrieval using MSG-SEVIRI data, which further emphasizes the importance of satellite-based remote sensing in environmental monitoring.

Turner et al. (2003) proposed a framework for vulnerability analysis in sustainability science, which is essential for integrating the information derived from NDVI, NDBI, and LST monitoring into actionable insights for urban and environmental planning. This framework aids in understanding the broader implications of land cover changes on ecosystem vulnerability and sustainability.

The studies on vegetation indices and land cover change are vital for comprehensively understanding environmental dynamics and mitigating adverse climatic impacts. By using indices like NDVI, NDBI, and NDWI in conjunction with remote sensing data, researchers can effectively track and analyze changes in LST, informing better land-use practices and urban planning strategies to enhance environmental sustainability.

Fig. 2.

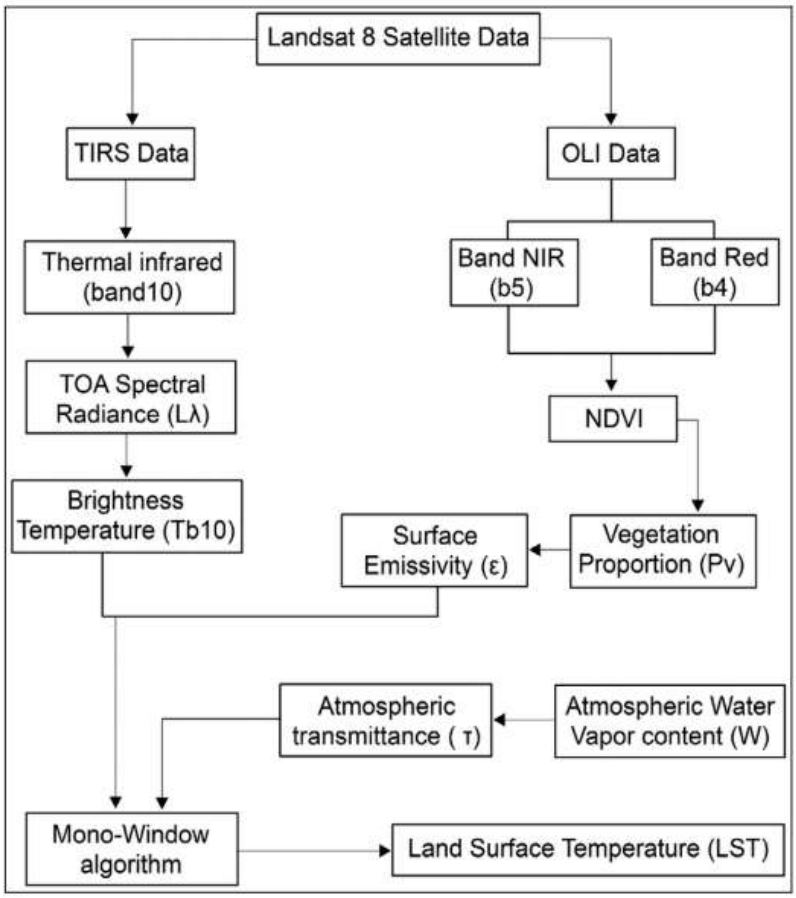

Steps to calculate the Land surface Temperature from Landsat 8 Data

Materials and Methods

The methodological framework and data sources for assessing land surface temperature (LST) dynamics, particularly in regions like the Himalayan terrain of Chamoli district, involve a robust integration of remote sensing techniques, GIS, and various datasets. This approach allows for precise mapping, monitoring, and interpretation of LST changes and their implications for vegetation cover. Remote sensing and GIS form the backbone of this methodological framework. Bhatta (2011) underscores the critical role of these technologies in environmental monitoring, providing detailed procedures for capturing and analyzing geospatial data. LST data retrieval relies heavily on satellite datasets such as those provided by NASA's Landsat program. The Thermal Infrared Sensor (TIRS) on Landsat satellites, mentioned on NASA's website, is particularly valuable for capturing thermal infrared data essential for LST analysis (NASA, 2019). Additionally, Duan et al. (2014) discuss the generation of time-consistent LST products from MODIS data, which highlights the importance of continuous and consistent data for accurate temporal analysis.

Vegetation indices and temperature data derived from MODIS (Didan, 2015) and other remote sensing products like Landsat are crucial for vegetation cover monitoring.

The utility of Landsat imagery in studying land cover and LST changes has been well-documented by Zhi-qiang and Qi-gang (2011), establishing the feasibility and accuracy of using Landsat data in such studies.

The summer season generally provides the strongest predictive capacity for Land Surface Temperature (LST), while winter offers the weakest. Many research indicates that the effects of land use/land cover (LULC) variables on predicting LST show consistent directions across seasons, though the magnitude of these effects varies seasonally. For instance, imperviousness is a consistent predictor of LST across all seasons, explaining about 50% of the total variation in winter and up to 77.9% in summer. Vegetation-related variables, especially tree canopy, are effective LST predictors during summer and fall, significantly contributing to LST reduction.

The most recent in the NRSA Landsat series is Landsat 8. The Earth Explorer website offers free access to data. Landsat 8 OLI-TIRS with meta data (MTL) file for the study area (Path/Row – 145 / 039) and Landsat 5-7 data for the year 2025, 2020, 2010, 2000, and 1990 have been collected from the USGS Earth Explorer website, fig 2 is showing the step by step method. In this study, the year-wise data from 1990 to 2025 has been collected with

an interval of 10 years and for each year, seasonal (Summer, winter, and rainy season) images have been collected to estimate LST and compute NDVI. Three separate maps have been generated for each of the seasons (Summer, Monsoon, Winter). Mono window algorithm approach has been adopted for the to calculate the Land Surface Temperature of the study area with the help of Arc GIS 10.6.1 software. Vegetation percentage, emissivity, and Land surface Temperature all have been done by following steps,

Methodology used: surface covers i.e. vegetation cover, barren land, water bosies, build-up land, etc. are distinguishable in standard false colour composite that is RGB 4,3,2. Table 1 is showing the formula to calculate the NDVI, and NDBI from various landsat data.

Table 1. Formula of NDVI, NDBI from Landsat 4-8 data

Indices	**Formula**	**Landsat 8 band Used**	**Landsat 7 or 4-5 band used**
Normalized Difference Vegetation Index (NDVI)	NDVI = (NIR – Red) / (NIR + Red)	NDVI = (Band 5 – Band 4) / (Band 5 + Band 4)	NDVI = (Band 4 – Band 3) / (Band 4 + Band 3)
Normalized Difference Build up Index (NDBI)	NDBI = (SWIR – NIR) / (SWIR + NIR)	NDBI = (Band 6 – Band 5) / (Band 6 + Band 5)	NDBI = (Band 5 – Band 4) / (Band 5 + Band 4)

Calculation of Land Surface Temperature from Landsat 8 data: Table 2 and 3 are showing the metadata for the calculation of LST from Landsat 4-8 imageries.

LST = (BT / (1 + (0.00115 * BT / 1.4388) * Ln(ε)))

(BT/ (1 + (10.895 * BT) / 14388 * Ln (ε))

Calculation of TOA (Top of Atmospheric) spectral radiance.

TOA (L) = ML * Qcal + AL

where:

ML = Band-specific multiplicative rescaling factor from the metadata (RADIANCE_MULT_BAND_x, where x is the band number).

Qcal = corresponds to band 10.

AL = Band-specific additive rescaling factor from the metadata (RADIANCE_ADD_BAND_x, where x is the band number).

Correction value of Band 10 = 0.29

TOA = 0.0003342 * "Band 10" + 0.1-0.29

Brightness Temperature conversion

BT = (K2 / (ln (K1 / L) + 1)) − 273.15

K1 = Band-specific thermal conversion constant from the metadata (K1_CONSTANT_BAND_x, where x is the thermal band number).

K2 = Band-specific thermal conversion constant from the metadata (K2_CONSTANT_BAND_x, where x is the thermal band number).

L = TOA

Therefore, to obtain the results in Celsius, the radiant temperature is adjusted by adding the absolute zero (approx. -273.15°C).

BT = (1321.0789 / Ln ((774.8853 / "%TOA%") + 1)) – 273.15

NDVI = (Band 5 – Band 4) / (Band 5 + Band 4)

Calculate the proportion of vegetation Pv

Pv = Square ((NDVI – NDVImin) / (NDVImax – NDVImin))

Pv = Square(("NDVI" – 0.216901) / (0.632267 – 0.216901))

Calculate Emissivity ε

ε = 0.004 * Pv + 0.986

Calculation of Land Surface Temperature (Landsat 5-7):

Conversion DN to Radiance

$$L_\lambda = \left(\frac{LMAX_\lambda - LMIN_\lambda}{QCALMAX - QCALMIN}\right) \cdot (QCAL - QCALMIN) + LMIN_\lambda$$

Covert Radiance into BT (In Kelvin)

$$T = \frac{K2}{\ln\left(\frac{K1}{L_\lambda} + 1\right)}$$

Convert Degree Kelvin into Degree Celsius

C=K-273.15

Table 2. Metadata of TIRS and OLI (Landsat 8, Landsat 4-7)

Details of Metadata of TIRS and OLI (Landsat 8, Landsat 4-7)	**2025**		**2020**	
Sensor	OLI	TIRS	OLI	TIRS
Date of Acquisition	2025-05-23		2020-05-25	
Sun Elevation	68.42668260		68.59794333	
Path/Row	145/39		145/39	
Band	9	2	9	2
Resolution	30 m	100 m	30 m	100 m
Radiance-Mult-Band-10	:	3.3420E-04	:	3.3420E-04
Radiance-Mult-Band-11	:	3.3420E-04	:	3.3420E-04
Radiance-Add-Band-10	:	0.10000	:	0.10000
Radiance-Add-Band-11	:	0.10000	:	0.10000
K_1 for Band 10	:	774.8853	:	774.8853
K_1 for Band 11	:	480.8883	:	480.8883
K_2 for Band 10	:	1321.0789	:	1321.0789
K_2 for Band 11	:	1201.1442	:	1201.1442

Table 3. Metadata for the calculation of LST

Details of Metadata of TIRS and OLI (Landsat 8, Landsat 4-7)	**2010**	**2000**	**1990**
Sensor	TM	TM	TM
Date of Acquisition	2010-05-22	2000-05-10	1990-03-04
Sun Elevation	66.82788495	65.41171305	40.18636694
Path/Row	145/039	145/039	145/039
Band	8	8	7
Resolution	30m	30m	30m
Radiance-Max-Band-6	12.650	12.650	15.303
Radiance-Min-Band-6	3.200	3.200	1.238
Quantize-Cal-Max-Band 6	255	255	255
Quantize-Cal-Min-Band 6	1	1	1
K_1 for Band 6	666.09	666.09	607.76
K_2 for Band 6	1282.71	1282.71	1260.56

Results and Discussion

The fluctuation in surface temperature of various surface patterns is shown by the thermal energy radiated by the earth's surface, which influences aspects such various land use types, plant cover, and soil in the research region. Changes in surface temperature regulate how much heat and water are exchanged with the atmosphere, which leads to climatic change in the area. Although some climatic phenomena are minor contributors to temperature variation, other factors, such as the rapid development of tourism, the conversion of land, kitchen firewood combustion, periodic removal of firewood, such as eucalyptus, and the replacement of forests with settlements and restaurants, among others, play a larger part. Data from remote sensing technologies, like as Landsat 8 TIRS, has proven to be useful for estimating LST. The findings allow us to make more accurate estimates of the study area's microclimate, hot spots, and most temperature-vulnerable places, as well as to take the appropriate scientific

steps to slow the rise in temperature, such as planting trees, inspecting cars often for pollution, reducing the amount of plastic that is burned, etc.

Landsat 8 TIRS and OLI images with meta data (MTL) file for the study area (Path/Row – 145 / 039) and Landsat 5-7 data for the year 2025, 2020, 2010, 2000, and 1990 have been downloaded from USGS Earth Explorer website. The images were already rectified to WGS-1984-UTM-Zone_44N. The next step involved is the conversion of DN (Digital Number) to the physical measure of Top of Atmospheric Reflectance (TOA) given in the metadata file and the Thermal band to At-Satellite Brightness Temperature. The file with the extension. MTL provided in the Landsat 8 image set contains the thermal constants needed to convert TIRS data to the at-satellite brightness temperature. TIRS band data is used to convert spectral radiance to brightness temperature by processing thermal constants provided in the metadata file.

The provided Land Surface Temperature (LST) data for Chamoli District between 1990 and 2025 reveals a discernible warming trend, particularly in the minimum and mean summer temperatures. Fig. 3 and Table 4 show that the minimum temperature has notably increased from $-40.96 \circ C$ in 1990 to $-22.93 \circ C$ in 2025, suggesting a reduction in extreme cold events, which could influence the length of the growing season and alter vegetation patterns. While the maximum temperatures show some variability, peaking at $48.93 \circ C$ in 2010 before a slight decrease, the overall trajectory of mean temperatures indicates a warmer environment over the decades. The consistently high standard deviation values across all years point to significant spatial and temporal heterogeneity in LST within the district, which could be attributed to diverse topographical features, land use patterns, or varying responses of different land covers to climatic shifts.

Table 4. Land Surface Temperature Values

Year of Acquisition		**Minimum Temperature (ºC)**	**Maximum Temperature (ºC)**	**Mean Temperature (ºC)**	**Standard Deviation**
2025	Summer	-22.93	40.81	13.25	10.36
2020	Summer	-19.87	45.68	15.76	12.56
2010	Summer	-24.27	48.93	17.32	13.35
2000	Summer	-25.62	47.04	12.04	11.05
1990	Summer	-40.96	25.82	-4.33	13.37

Fig 3

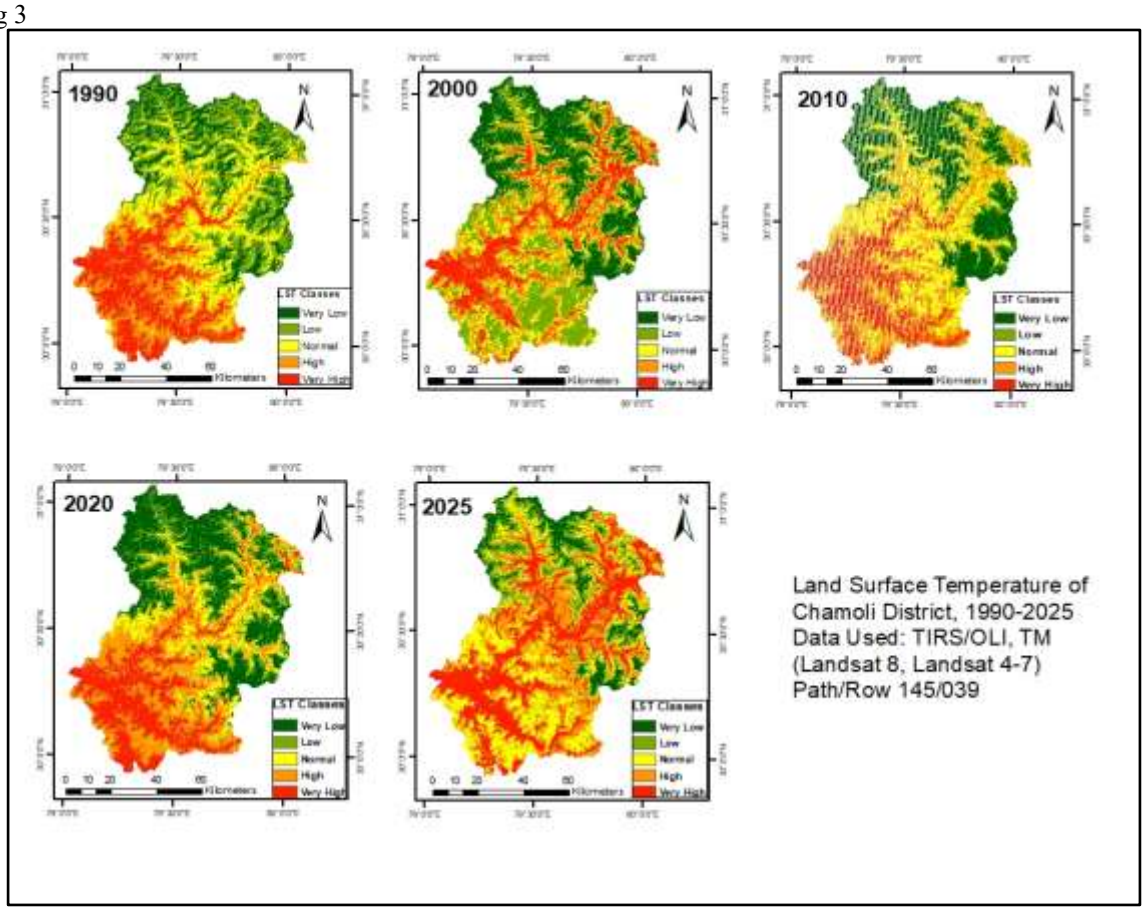

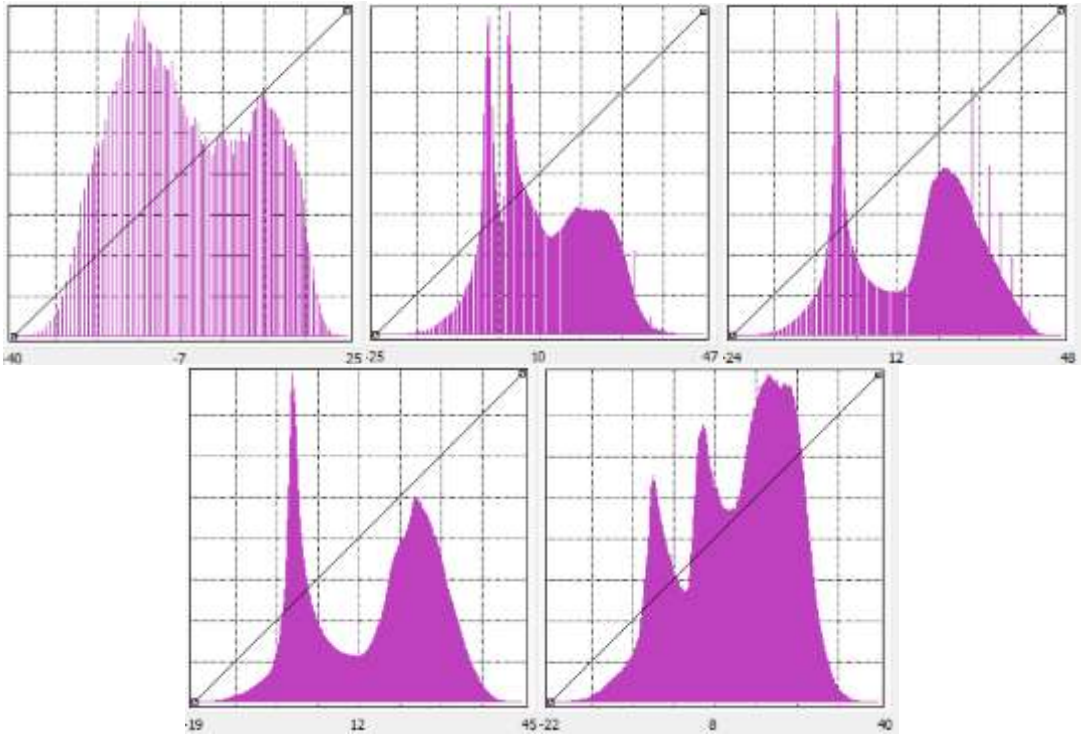

This observed warming trend and temperature variability carry significant implications for the vegetation cover in Chamoli District. Higher minimum temperatures may lead to earlier spring thaws and extended periods of growth, but simultaneously, increased mean and potentially maximum temperatures could exacerbate water stress, especially for vegetation not adapted to warmer conditions. Such changes can directly influence plant phenology, species distribution, and overall ecosystem health. The spatial variability in LST, as indicated by the standard deviation, suggests that some areas may be experiencing more pronounced warming or heat stress than others, potentially leading to localized vegetation degradation or shifts in dominant plant species. Therefore, a comprehensive understanding of these temperature dynamics is essential for predicting and mitigating the impacts on the region's diverse vegetation.

The value of NDVI is ranges between -1 to 1. High near infrared can be estimated by the high value of NDVI which is a clear indication of dense vegetation, and negative value represents water bosy. In the table below, the result has been depicted in a clear format. Table 5 is showing the NDVI classes based on the range of NDVI values, Fig 4

Table 5. NDVI Feature classes based on NDVI Valus calculated in ArcGIS

NDVI Value	Feature represents
-1 to 0	Water bodies
-0.1 to 0.1	Snow cover, barren land, sand, etc.
0.2 to 0.5	Grass land, or shrubs
0.6 to 1.0	Dense vegetation cover

Build-up Index is the index for analysis of urban pattern using NDBI and NDVI. Built-up index is the binary image with only higher positive value indicates built-up and barren thus, allows BU to map the built-up area automatically, Fig 5.

Fig. 4

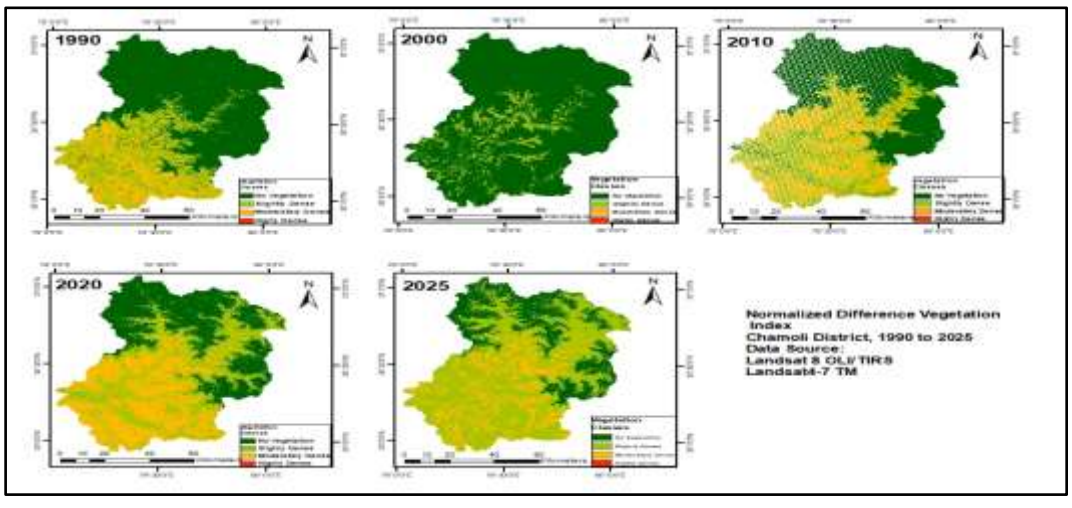

Fig 5

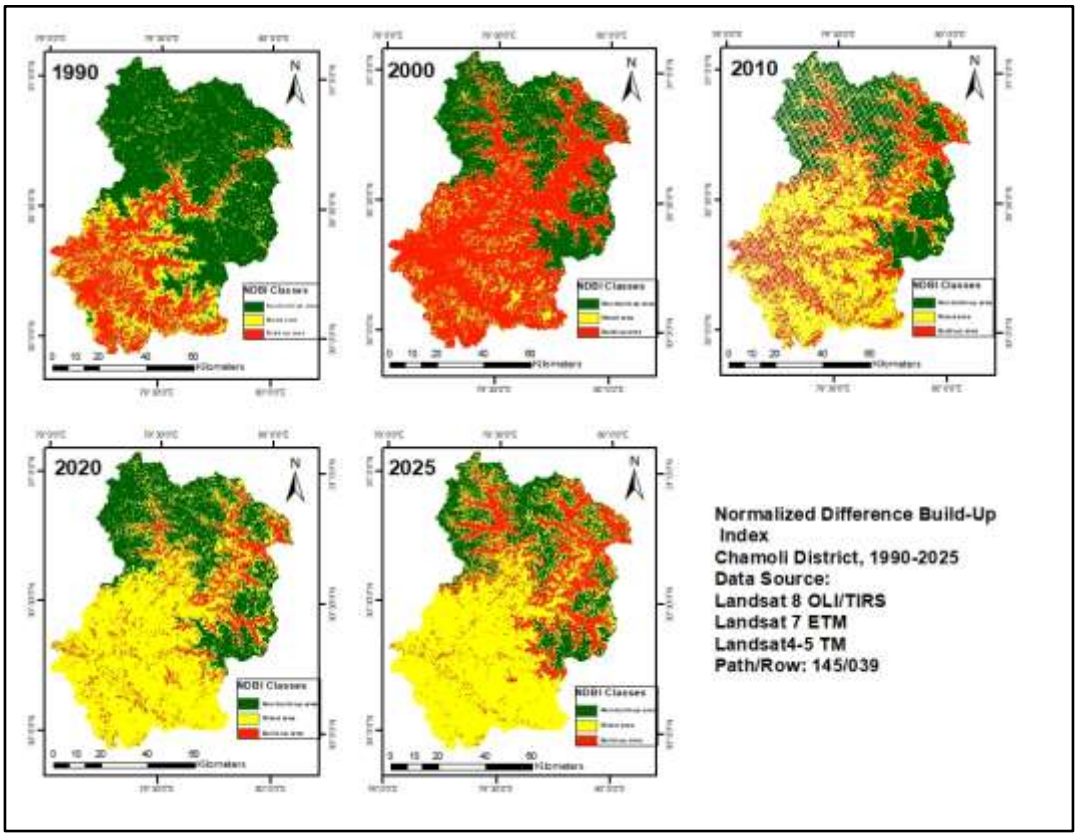

To further investigate these findings, two primary objectives for a study on "Assessment of Land Surface Temperature Dynamics of Chamoli District Using Landsat Data: Implications for Vegetation Cover Monitoring" would be to: 1) analyze the temporal trends and spatial variability of Land Surface Temperature (LST) in Chamoli District during summer seasons from 1990 to 2025 using Landsat satellite data, and 2) assess the impact of these LST dynamics on local vegetation cover changes and evaluate the implications for ecological health and climate adaptation planning. These objectives would enable a detailed exploration of the relationship between temperature shifts and vegetation response, providing crucial insights for environmental management and conservation efforts in the region.

References

1. Alademomi, A. S., Okolie, C. J., Daramola, O. E., Akinnusi, S. A., Adediran, E., Olanrewaju, H. O., Alabi, A. O., Salami, T. J., & Odumosu, J. (2022). The interrelationship between LST, NDVI, NDBI, and land cover change in a section of Lagos metropolis, Nigeria. *Applied Geomatics*. https://doi.org/10.1007/s12518-022-00399-8
2. Aires, F., Prigent, C., Rossow, W. B., & Rothstein, M. A new neural network approach including first guess for retrieval of atmospheric water vapor, cloud liquid water path, surface temperature, and emissivities over land from satellite microwave observations. Journal of Geophysical Research, (2001), 106 (D14) 14887–14907.
3. Anderson, M. C., Norman, J. M., Kustas, W. P., Houborg, R., Starks, P. J., & Agam, N., A thermal-based remote sensing technique for routine mapping of land-surface carbon, water and energy fluxes from field to regional scales. Remote Sensing of Environment, (2008), 112, 4227–4241.
4. Arnfield, A. J., Two decades of urban climate research: a review of turbulence, exchanges of energy and water, and the urban heat island. International Journal of Climatology, (2003) 23 1–26.
5. Avashia, V., Garg, A., Dholakia, H., 2021. Understanding temperature related health risk in context of urban land use changes. Landsc. Urban Plan. 212, 104107. https://doi.org/10.1016/j.landurbplan.2021.104107.
6. Ayse Dagliyar, Ugur Avdan, Nalan Demircioglu Yildiz and Hakan A. Nefeslioglu, (2015), Geophysical Research, Abstracts, Vol.17, EGU, General Assembly
7. Barnes, K.B., Morgan III, J.M., Roberge, M.C. and Lowe, S. (2001) Sprawl Develop-ment: Its Patterns, Consequences, and Measurement. Towson University, Towson.
8. Bastiaanssen, W. G. M., Menenti, M., Feddes, R. A., & Holtslag, A.A.M., A remote sensing surface energy balance algorithm for land (SEBAL) Formulation. Journal of Hydrology, (1998) 212 198–212
9. Bendib, A., Dridi, H., & Kalla, M. I. (2016). Contribution of Landsat 8 data for the estimation of land surface temperature in Batna city, Eastern Algeria. *Geocarto International*. https://doi.org/10.1080/10106049.2016.1156167
10. Berk, A, Anderson, G.P., Acharya, P.K., Chetwynd, J.H., Bernstein, L.S., Shettle, E.P., Matthew, M.W., and Adler-Golden, J.H., 1999, MODTRAN 4 users manual, report. Air Force Research Laboratory Space Vehicles Directorate, Hascom AFB, Mass.
11. Bhatta, B. (2011). Remote sensing and GIS: Second edition. New Delhi, India: Oxford University Press.

12. Bhatta, B., Saraswati, S. and Bandopadhyay, D. (2010) Urban Sprawl Measurement from Remote Sensing Data. *Applied Geography*, 30, 731-740.
13. Bilal, H., Chamhuri, S., Mokhtar, M.B., Kanniah, K.D., 2019. Recent snow cover variation in the upper Indus basin of Gilgit Baltistan, Hindukush Karakoram Himalaya. J. Mt. Sci. 16 (2), 296–308.
14. Bolch, T., Kulkarni, A., Huggel, C., Paul, F., Cogley, J.G., Frey, H., Kargel, J.S., Fujita, K., Scheel, M., Bajracharya, S., Stoffel, M., 2012. The State and Fate of Himalayan Glaciers. Science 336 (6079), 310–314. https://doi.org/ 10.1126/science.1215828.
15. Bolch, T., Shea, J.M., Liu, S., Azam, F.M., Gao, Y., Gruber, S., Immerzeel, W.W., Kulkarni, A., Li, H., Tahir, A.A., Zhang, G., Zhang, Y., 2019. Status and change of the cryosphere in the Extended Hindu Kush Himalaya Region. In: Wester,
16. Briassoulis H. (2000). Analysis of Land Use Change: Theoretical and Modelling Approaches. The Web Book of Regional Science, Scott Loveridge, ed. Regional Research Institute, West Virginia University, USA <http://www.rri.wvu.edu/WebBook/Briassoulis/ contents.htm>.
17. Brunori, E., Salvati, L., Mancinelli, R., Smiraglia, D., Biasi, R., 2017. Multi-temporal land use and cover changing analysis: the environmental impact in Mediterranean area. Int. J. Sustain. Dev. World Ecol. 24 (3), 276–288. https://doi.org/10.1080/ 13504509.2016.1205156.
18. Brunsell, N.A., & Gillies, R.R, Length scale analysis of surface energy fluxes derived from remote sensing. *Journal of Hydrometeorology*, (2003)4 1212–1219.
19. Cantika, L. D. A., Saraswati . R., Wibowo, A. (2020) The Effect of NDVI and NDBI on Land Surface Temperature in Cirebon City 2015 and 2019. E3S Web of Conferences, 202, 13006 (2020)
20. Census of Idukki District (2011), Census of India, New Delhi
21. Chen, B., Liu, Z., 2016. Global water vapor variability and trend from the latest 36 year (1979 to 2014) data of ECMWF and NCEP reanalyses, radiosonde, GPS, and microwave satellite. J. Geophys. Res. Atmos. 121 (19), 11–442.
22. Chen, C., Park, T., Wang, X., Piao, S., Xu, B., Chaturvedi, R.K., Fuchs, R., Brovkin, V., Ciais, P., Fensholt, R., Tømmervik, H., Bala, G., Zhu, Z., Nemani, R.R., Myneni, R.B., 2019. China and India lead in greening of the world through land-use management. Nat. Sustain 2 (2), 122–129.
23. Chunyang He, Peijun Shi, Dingyong Xie & Yuanyuan Zhao (2010). Improving the normalized difference build-up index to map urban built-up areas using a semiautomatic segmentation approach, Remote Sensing Letters, 1:4, 213-221, DOI: 10.1080/01431161.2010.481681
24. Coll, C., Caselles, V., Galve, J.M., Valor , E., Niclòs, R., and Sánchez, J.M., Evaluation of split-window and dual-angle correction methods for land surface temperature retrieval from Envisat/AATSR data. Journal of Geophysical Research, 111, 12105 doi 10.1029/2005JD006830, 2006.
25. Coll, C., Caselles, V., Galve, J.M., Valor , E., Niclòs, R., Sánchez, J.M. and Rivas R., Ground measurements for the validation of land surface temperatures derived from AATSR and MODIS data, Remote Sensing of Environment, 97, 288-300, 2005.
26. Coll, C., Caselles, V., Valor , E., Niclòs, R., Sánchez, J.M., Galve, J.M. and Mira M., Temperature and emissivity separation from ASTER data for low spectral contrast surfaces. Remote Sensing of Environment, 110, 162-175, 2007.
27. Conrad, O., Bechtel, B., Bock, M., Dietrich, H., Fischer, E., Gerlitz, L., Wehberg, J., Wichmann, V., Böhner, J., 2015. System for automated geoscientific analyses (SAGA) v. 2.1.4. Geosci. Model. Dev. 8 (7), 1991–2007.
28. Crippen, R.E. (1990). Calculating the vegetation index faster: Remote sensing of Enviromnment, 34, 71-73.
29. Department of Hydrology and Meteorology (DHM), 2017. Observed Climate Trend Analysis of Nepal. Department of Hydrology and Meteorology, Nepal.
30. Desinayak, N., Prasad, A.K., El-Askary, H., Kafatos, M., Asrar, G.R., 2021. Snow cover variability and trend over Hindu Kush Himalayan region using MODIS and SRTM data. Ann. Geophys. Discuss., 1–24
31. Didan, K., 2015. MOD13C2 MODIS/Terra Vegetation Indices Monthly L3 Global 0.05Deg CMG V006. NASA EOSDIS Land Processes DAAC.
32. Dimri, A.P., 2021. Decoding the Karakoram Anomaly. Sci. Total Environ. 788, 147864. https://doi.org/10.1016/j.scitotenv.2021.147864.
33. Duan, S.-B., Li, Z.-L., Li, H., Göttsche, F.-M., Wu, H., Zhao, W., Leng, P., Zhang, X., Coll, C., 2019. Validation of Collection 6 MODIS land surface temperature product using in situ measurements. Remote Sens. Environ. 225, 16–29.
34. Du, C., Ren, H., Qin, Q., Meng, J., & Zhao, S. (2015). A practical split-window algorithm for estimating land surface temperature from Landsat 8 data. Remote Sensing, 7(1), 647-665. https://doi.org/10.3390/rs70100647
35. Duan, S.-B.; Li, Z.-L.; Tang, B.-H.; Wu, H.; Tang, R.L. Generation of a time-consistent land
36. Earthdata Search, 2019. Greenbelt, MD: Earth Science Data and Information System (ESDIS) Project, Earth Science Projects Division (ESPD). Flight Projects Directorate, Goddard Space Flight Center (GSFC) National Aeronautics and Space Administration (NASA). https://search.earthdata.nasa.gov/.
37. Fuqin Li, Thomas J. Jackson, William P. Kustas, Thomas J. Schmugge, Andrew N. French, Michael H. Cosh, Rajat Bindlish (2004), "Deriving Land Surface Temperature from Landsat 5 and 7 during SMEX02/SMACEX, Remote Sensing of Environment 92, 521-534, Elsevier.
38. Galve J.M., C. Coll, V. Caselles and E. Valor, An Atmospheric Radiosounding database for generating Land Surface Temperature algorithms. IEEE Transactions on Geoscience and Remote Sensing, 2008 (in press)
39. Gao, J., 2019. Global population projection grids based on Shared Socioeconomic Pathways (SSPs), downscaled 1-km grids, 2010–2100. Palisades, NY. doi.org/ 10.7927/H44747X4.

40. Gao, Y., Chen, F., Lettenmaier, D.P., Xu, J., Xiao, L., Li, X., 2018. Does elevationdependent warming hold true above 5000 m elevation? Lessons from the Tibetan Plateau. NPJ Clim. Atmos. Sci. 1 (1), 1–7.
41. Gao. "NDWI—A normalized difference water index for remote sensing of vegetation liquid water from space." 1996.
42. Hall, D.K., Riggs, G.A., 2015. MODIS/Terra Snow Cover Monthly L3 Global 0.05Deg CMG, Version 6. NASA National Snow and Ice Data Center Distributed Active Archive Center, Boulder, CO.
43. Hashim, H., Latif, Z., A., Adnan, N. A. (2019). Urban Vegetation Classification with NDVI Threshold Value Method with Very High Resolution (VHR) Pleiades Imagery. *The International Archives of the Photogrammetry, Remote Sensing and Spatial Information Sciences*, Volume XLII-4/W16, 237-340
44. Held, I.M., Soden, B.J., 2000. Water vapor feedback and global warming. Annu. Rev. Energy Environ 25 (1), 441–475.
45. Hereher, M.E., 2019. Estimation of monthly surface air temperatures from MODIS LST time series data: application to the deserts in the Sultanate of Oman. Environ. Monit. Assess. 191 (9), 1–11
46. http://landsat.gsfc.nasa.gov/?p=1940, https://doi.org/ 10.5067/MODIS/MOD13C2.006.
47. Huang, S., Tang, L., Hupy, J., Shao, G., (2020). A commentary review on the use of normalized difference vegetation index (NDVI) in the era of popular remote sensing. J. For. Res. 31 (5) https://doi.org/10.1007/s11676-020-01155-1.
48. Jackson, R. D., S. B. Idso, R. J. Reginato, and P. J. Pinter Jr., Canopy temperature as a crop water stress indicator, Water Resour. Res., (1981) 17, 1133–1138
49. Jiang, G.M., Li, Z.L. & Nerry, F., Land surface emissivity retrieval from combined mid-infrared and thermal infrared data of MSG-SEVIRI. Remote Sensing of Environment, (2006)105 326–340.
50. John R. Jenson (2009), "Remote Sensing of the Environment An Earth Resource Perspective", Second Edition, Dorling Kindersley, Delhi
51. Kalma, J. D.,McVicar, T. R., &McCabe,M. F., Estimating land surface evaporation: A review of methods using remotely sensed surface temperature data. Surveys in Geophysics, (2008) 29, 421–469
52. Karnam, H. K. (2018). Study of Normalized Difference Built-up (NDBI) Index in Automatically Mapping Urban Areas from Landsat Imagery. International Journal of Scientific Research and Review, 7(1), Retrived from: https://www.researchgate.net/publication/339230287
53. Karnieli, A., Agam, N., Pinker, R. T., Anderson, M., Imhoff, M. L., & Gutman, G. G. Use of NDVI and land surface temperature for drought assessment: Merits and limitations. Journal of Climate, (2010), 23, 618–633
54. Kogan, F. N., Operational space technology for global vegetation assessment, Bulletin of the American Meteorological Society, (2001)82 1949–1964.
55. Kustas, W., & Anderson, M. Advances in thermal infrared remote sensing for land surface modeling, Agricultural and Forest Meteorology, (2009), 149, 2071–2081.
56. Manat SRIVANIT, (2012) "Assessing the Impact of Urbanization on Urban Thermal Environment: A case study of Bangkok metropolitan", International Journal of Applied Science and Technology, Vol.2, No. 7.
57. Moran, M. S., Clarke, T. R., Inoue, Y., &. Vidal, A., Estimating crop water deficit using the relation between surface air temperature and spectral vegetation index. Remote Sens. Environ., (1994)49, 246–263
58. Niclòs, R., Valiente, J.A., Barberà, M.J., Estrela, M.J., Galve, J.M. & Caselles, V., Preliminary results on the retrieval of land surface temperature from MSG-SEVIRI data in Eastern Spain, in EUMETSAT 2009: Proceedings of Meteorological Satellite Conference (2009) 21-25.
59. P., Mishra, A., Mukherji, A., Shrestha, A.B. (Eds.), The Hindu Kush Himalaya Assessment: Mountains, Climate Change, Sustainability and People. Springer International Publishing, Cham, pp. 209–255. https://doi.org/10.1007/978-3- 319-92288-1_7.
60. Peng, J., Ma, J., Liu, Q., Liu, Y., Hu, Y., Li, Y., & Yue, Y. (2018). Spatial-temporal change of land surface temperature across 285 cities in China: An urban-rural contrast perspective. *The Science of the total environment*, *635*, 487–497. https://doi.org/10.1016/j.scitotenv.2018.04.105
61. Peng, X., Wu, W., Zheng, Y., Sun, J., Hu, T., & Wang, P. (2020). Correlation analysis of land surface temperature and topographic elements in Hangzhou, China. *Scientific Reports*, *10*, 10851. https://doi.org/10.1038/s41598-020-67423-6
62. Pradsad Rajendran, Mani. K (2015), "Estimation of Spatial Variability of Land Surface Temperature using Landsat 8 Imagery", The International Journal of Engineering And Science (IJES), Volume 4, Issue-11, pp-19-23.
63. Rajeshwari A and Mani ND (2014), "Estimation of Land Surface Temperature of Dindigul District using Landsat 8 Data", IJRET: International Journal of Research in Engineering and Technology, Vol.03, Issue.05.
64. Rani, S., & Mal, S., (2022), Trends in land surface temperature and its drivers over the High Mountain Asia. *The Egyptian Journal of Remote Sensing and Space Sciences*, 25 (2022) 717–729
65. Rodell, M., & Coauthors, The global land data assimilation system. Bull. Amer. Meteor. Soc., (2004) 85 381–394.
66. Rubio, E., Caselles, V., Coll, C., Valor, E., and Sospedra, F., "Thermal-infrared emissivities of natural surfaces: Improvements on the experimental set-up and new measurements". International Journal of Remote Sensing, 24(24), 5379– 5390, 2003.
67. Sajib, M. Q. U., & Wang, T. (2020). Estimation of Land Surface Temperature in an Agricultural Region of Bangladesh from Landsat 8: Intercomparison of Four Algorithms. *Sensors*, *20*(6), 1778. MDPI AG. Retrieved from http://dx.doi.org/10.3390/s20061778
68. Shetri, T. (2018). NDVI, NDBI & NDWI Calculation Using Landsat 7, 8 Retrieved from:

https://www.linkedin.com/pulse/ndvi-ndbi-ndwi-calculation-using-landsat-7-8-tek-bahadur-kshetri/
69. Su, Z., The Surface Energy Balance System (SEBS) for estimation of turbulent heat fluxes. Hydrology and Earth System Sciences, (2002)6 85–100.
70. Sun, D., & Pinker, R.T., Estimation of land surface temperature from a Geostationary Operational Environmental Satellite (GOES-8). Journal of Geophysical Research, (2003)108, 43-26.
71. Suresh. S, Ajay Suresh and Mani. K (2015), "Analysis of land surface temperature variation using thermal remote sensing spectral data of Landsat satellite in Devikulam Taluk, Kerala-India", IJREAS, Volume 5, Issue 5, PP: 145-154.
72. Surface temperature product from MODIS data. *Remote Sens. Environ*. 2014, 140, 339–349
73. Turner et al. 2003. A framework for vulnerability analysis in sustainability science. Proc. Nat. Acad. Sci. 100 (14): 8074-8079.
74. Voogt, J. A., & Oke, T. R., Thermal remote sensing of urban climates, Remote Sensing of Environment, (2003) 86, 370–384.
75. Weng, Q., Lu, D., & Schubring, J., Estimation of land surface temperature vegetation abundance relationship for urban heat island studies, Remote Sensing of Environment, (2004)89, 467–483.
76. Weng, Q., Thermal infrared remote sensing for urban climate and environmental studies: methods, applications, and trends. ISPRS Journal of Photogrammetry and Remote Sensing, (2009)64, 335–344.
77. Xu, H. (2007): Extraction of urban built-up land features from Landsat imagery using a thematic-oriented index combination technique. Photogrammetric Engineering & Remote Sensing. 73: 1381-1391
78. Xu, H. (2008) A New Index for Delineating Built-Up Land Features in Satellite Im-agery. International. *Journal of Remote Sensing*, 29, 4269-4276.Bugliarello, G. (2005) Large Urban Concentrations: A New Phenomenon. In: Read-er, A., Heiken, G., Fakundiny, R. and Sutter, J., Eds., Earth Science in the City, American Geophysical Union, New York, 7-19.
79. Y. Zha, J. Gao & S. Ni (2003) Use of normalized difference built-up index in automatically mapping urban areas from TM imagery, International Journal of Remote Sensing, 24:3, 583-594, DOI: 10.1080/01431160304987
80. Zhang, R., Tian, J., Su, H., Sun, X., Chen, S., & Xia, J., Two improvements of an operational two-layer model for terrestrial surface heat flux retrieval. Sensors, (2008), 8, 6165–6187
81. Zheng, Y., Tang, L., Wang, H. (2021). An improved approach for monitoring urban built-up areas by combining NPP-VIIRS nighttime light, NDVI, NDWI, and NDBI. *Journal of Cleaner Production*, 328, Retrived from: Journal of Cleaner Production | Vol 328, 15 December 2021 | ScienceDirect.com by Elsevier
82. Zhi-qiang LV, Qi-gang Zhou (2011), "Utility of Landsat Image in the study of Land Cover and Land Surface Temperature Change", Sciverse Science Direct Procedia Environmental Sciences 1287
83. Assessing seasonal dynamics of land surface temperature (LST … (n.d.). https://www.sciencedirect.com/science/article/pii/S2666016423002657
84. Comparison of the accuracy of daytime land surface temperature … (n.d.). https://www.sciencedirect.com/science/article/abs/pii/S1350449521000645
85. Correlation analysis of land surface temperature and topographic … (2020). https://pmc.ncbi.nlm.nih.gov/articles/PMC7320146/
86. Herb, W., Janke, B., Mohseni, O., & Stefan, H. (2008). Ground surface temperature simulation for different land covers. Journal of Hydrology. https://www.sciencedirect.com/science/article/pii/S0022169408002023
87. How to calculate seasonal mean land surface temperature (day time … (2022). https://www.researchgate.net/post/How_to_calculate_seasonal_mean_land_surface_temperature_day_time_using_satellite_images
88. Hulley, G., Ghent, D., Göttsche, F., Guillevic, P., Mildrexler, D. J., & Coll, C. (2019). Land Surface Temperature. Taking the Temperature of the Earth. https://www.semanticscholar.org/paper/3c6c8251617210578b69ff081f82309191d90d58
89. Impacts of land surface temperature and ambient factors on near … (2025). https://www.sciencedirect.com/science/article/abs/pii/S2210670725001349
90. Janatian, N., Sadeghi, M., & Sanaeinejad, S. (2017). A statistical framework for estimating air temperature using MODIS land surface temperature data. https://rmets.onlinelibrary.wiley.com/doi/abs/10.1002/joc.4766
91. Kalma, J., McVicar, T., & McCabe, M. (2008). Estimating land surface evaporation: A review of methods using remotely sensed surface temperature data. Surveys in Geophysics. https://link.springer.com/article/10.1007/s10712-008-9037-z
92. Kim, S., & Lee, Y. (2020). Improvement of satellite-based land surface temperature estimation. https://www.semanticscholar.org/paper/ab546d0c2664d7d3b192dc90e6e166eba8111a97
93. Land surface and air temperature dynamics: The role of urban form … (2023). https://www.sciencedirect.com/science/article/pii/S0048969723059338
94. Land Surface Temperature | NASA Earthdata. (n.d.). https://www.earthdata.nasa.gov/topics/land-surface/land-surface-temperature
95. Land Surface Temperature | VTANR Open Data. (n.d.). https://anrgeodata.vermont.gov/pages/78cb2f75bfda4848bb3304e703b8af5a
96. Land Surface Temperature - an overview | ScienceDirect Topics. (n.d.). https://www.sciencedirect.com/topics/earth-and-planetary-sciences/land-surface-temperature
97. Land Surface Temperature - NASA Earth Observatory. (2025). https://earthobservatory.nasa.gov/global-maps/MOD_LSTD_M

98. Land Surface Temperature Comparison | Sentinel Hub custom scripts. (n.d.). https://custom-scripts.sentinel-hub.com/custom-scripts/landsat-8/land_surface_temperature_comparison/
99. Land Surface Temperature Data Generation. (2019). Techniques and Methods in Urban Remote Sensing. https://www.semanticscholar.org/paper/28e9d9b6f4206b04f3ddefcf06fda0a4ff69acf3
100. Land-surface temperature (LST) calculation process with equation… (n.d.). https://www.researchgate.net/figure/Land-surface-temperature-LST-calculation-process-with-equation-descriptions_tbl2_335176595
101. Local hourly trends in near-surface and land surface temperatures. (2025). https://www.nature.com/articles/s41598-025-15731-0
102. MODIS land surface temperature in East Antarctica: accuracy and its … (2024). https://www.cambridge.org/core/journals/journal-of-glaciology/article/modis-land-surface-temperature-in-east-antarctica-accuracy-and-its-main-affecting-factors/5C0643A417993EF24B346673B4F4ECC5
103. Nguyen, Q. K., Trinh, L., Dao, K., & Dang, N. D. (2019). Land Surface Temperature Dynamics In Dry Season 2015-2016 According To Landsat 8 Data In The South-East Region of Vietnam. GEOGRAPHY, ENVIRONMENT, SUSTAINABILITY. https://www.semanticscholar.org/paper/667a698cc8c15f17858e1077ec7236eb222c7a8f
104. Peng, J., Jia, J., Liu, Y., Li, H., & Wu, J. (2018). Seasonal contrast of the dominant factors for spatial distribution of land surface temperature in urban areas. Remote Sensing of Environment. https://www.sciencedirect.com/science/article/pii/S003442571830289X
105. Rasheed, M. U., Mahmood, S. A., Khan, R. M. A., & Sohl, M. A. (2023). LS8pyCalc: semi-automated Python calculator to retrieve land surface temperature, cross verified through in situ and MODIS datasets. Arabian Journal of Geosciences. https://www.semanticscholar.org/paper/7c5fcff0e7df677effe35c595f7c0b219f256f90
106. Rosado, R. M. G., Guzmán, E. A., Lopez, C. J. E., Molina, W. M., Garcia, H. L. C., & Yedra, E. L. (2020). Mapping the LST (Land Surface Temperature) with Satellite Information and Software ArcGis. IOP Conference Series: Materials Science and Engineering. https://www.semanticscholar.org/paper/b47d6861d85c4dc881a6ea8ad4d7081eb225ed85
107. Satellite Remote Sensing of Global Land Surface Temperature … (2022). https://agupubs.onlinelibrary.wiley.com/doi/full/10.1029/2022RG000777
108. Satellite-Based Land Surface Temperature for Deriving Growing … (2024). https://www.planet.com/pulse/satellite-based-land-surface-temperature-for-deriving-growing-degree-days/
109. Schwarzschild, K., & Planck, M. (2013). Earth's Surface Temperature. https://www.semanticscholar.org/paper/147ccfe9d18a1f9e2f0a96ca730525ff6d5f82d7
110. Sheng, Q., Zhang, Y., Li, K., Ling, X., & Li, J. (2024). Exploring the Seasonal Comparison of Land Surface Temperature Dominant Factors in the Tibetan Plateau. ISPRS Annals of the Photogrammetry, Remote Sensing and Spatial Information Sciences. https://www.semanticscholar.org/paper/dc267c282ee506a82b247e275ce0d6e87564ef53
111. STAR - Land and Ocean Data Products - Land Surface Temperature. (2025). https://www.star.nesdis.noaa.gov/goesr/product_land_lst.php
112. Tarawally, M., Xu, W., Kursah, M. B., & Kamara, A. (2021). Intra-seasonal variations in urban land surface temperature in two cities in Sierra Leone: the challenge of using a single-date image to represent a whole season. Spatial Information Research. https://www.semanticscholar.org/paper/cd91823bcb50149af1d5eb991c54066179cd9f70
113. Trigo, I., Monteiro, I., & Olesen, F. (2008). An assessment of remotely sensed land surface temperature. https://agupubs.onlinelibrary.wiley.com/doi/abs/10.1029/2008JD010035
114. Um, D. (2006). A Study on the Accuracy Improvement of Land Surface Temperature Extraction by Remote Sensing Data. https://www.semanticscholar.org/paper/fe111fa3061aae8726ed0a904b299f5c0ce93706
115. Xiaojuan, W. (2010). Method for Land Surface Temperature Retrieval. Geospatial Information. https://www.semanticscholar.org/paper/a5e8fe7e1507fd9d010cf17be2344b5fb8834b04
116. Yuan-sheng, Z., & Xia, G. (2004). STUDY ON THE INVERSION METHOD OF LAND SURFACE TEMPERATURE BY APPLYING IR BRIGHT TEMPERATURE DATA OF STILL SATELLITE. Northwestern Seismological Journal. https://www.semanticscholar.org/paper/0332e5feab4ad434f9eec76b576ef366b69ddc79
117. Zhi, Q. (2001). SPLIT WINDOW ALGORITHMS FOR RETRIEVING LAND SURFACE TEMPERATURE FROM NOAA-AVHRR DATA. Remote Sensing for Land & Resources. https://www.semanticscholar.org/paper/899d1dede60d50b167364794b52e1d5ac53a462d
118. Zhou, W., Qian, Y., Li, X., Li, W., & Han, L. (2014). … cover and the surface urban heat island: seasonal variability and effects of spatial and thematic resolution of land cover data on predicting land surface temperatures. Landscape Ecology. https://link.springer.com/article/10.1007/s10980-013-9950-5